

Application of Raman Spectroscopy for Studying Shocked Zircon from Terrestrial and Lunar Impactites: A Systematic Review

Dmitry A. Zamyatin

Mineral and Functional Material Physics Laboratory, Zavaritsky Institute of Geology and Geochemistry of the Ural Branch of the Russian Academy of Sciences, 620016 Ekaterinburg, Russia; zamyatin@igg.uran.ru; Tel.: +7-343-287-90-30

Abstract: A highly resistant mineral, zircon is capable of preserving information about impact processes. The present review paper is aimed at determining the extent to which Raman spectroscopy can be applied to studying shocked zircons from impactites to identify issues and gaps in the usage of Raman spectroscopy, both in order to highlight recent achievements, and to identify the most effective applications. **Method:** Following PRISMA guidelines, the review is based on peer-reviewed papers indexed in Google Scholar, Scopus and Web of Science databases up to 5 April 2022. Inclusion criteria: application of Raman spectroscopy to the study of shocked zircon from terrestrial and lunar impactites. **Results:** A total of 25 research papers were selected. Of these, 18 publications studied terrestrial impact craters, while 7 publications focused on lunar breccia samples. Nineteen of the studies were focused on the acquisition of new data on geological structures, while six examined zircon microstructures, their textural and spectroscopic features. **Conclusions:** The application of Raman spectroscopy to impactite zircons is linked with its application to zircon grains of various terrestrial rocks and the progress of the electron backscatter diffraction (EBSD) technique in the early 2000s. Raman spectroscopy was concluded to be most effective when applied to examining the degree of damage, as well as identifying phases and misorientation in zircon.

Keywords: zircon; impactites; Raman spectroscopy; radiation damage; microstructural deformations; orientation effect; polymorphs; impactites; systematic review

Citation: Zamyatin, D.A.

Application of Raman Spectroscopy for Studying Shocked Zircon from Terrestrial and Lunar Impactites: A Systematic Review. *Minerals* **2022**, *12*, 969. <https://doi.org/10.3390/min12080969>

Academic Editors: Elizaveta Kovaleva, Matthew Hube, Martin Clark and Jordi Ibanez-Insa

Received: 2 May 2022

Accepted: 23 July 2022

Published: 29 July 2022

Publisher's Note: MDPI stays neutral with regard to jurisdictional claims in published maps and institutional affiliations.



Copyright: © 2022 by the authors. Licensee MDPI, Basel, Switzerland. This article is an open access article distributed under the terms and conditions of the Creative Commons Attribution (CC BY) license (<https://creativecommons.org/licenses/by/4.0/>).

1. Introduction

Impactites are unique rocks in terms of the maximum possible pressures, temperatures and strain rate of processes occurring in planetary objects. Conditions during an impact process can reach hundreds of GPa and thousands of degrees Celsius in a few seconds (e.g., [1]). The process of meteorite impact cratering results in such effects as structural deformation, shock metamorphism, melting, and vaporization of the target materials [2]. While laboratory methods for creating such conditions are rather laborious and have limitations [3–5] (high cost of experiments, small sample volume, short melt transfer distances and short cooling times), the material from terrestrial impactites is quite easily accessible and opens up the possibility of studying the behavior of matter that had experienced extreme conditions (e.g., [1,2]). On the one hand, impactite minerals and glasses are of interest for material science as a high-entropy substance with potentially promising properties [6]. On the other hand, the study of terrestrial and lunar impact rocks leads to a better understanding of the processes of mineral formation at the early stages of Earth's formation, when impact metamorphism played a significant role in the development of the Earth's crust due to the large number of meteorite impacts. The study of the properties and composition of impactites makes it possible to determine the conditions under which deformations, transformation, melting, and evaporation of minerals occurred. A comparison of the data on the minerals of terrestrial and lunar impactites can reveal the

characteristic features of minerals from both planetary bodies due to the difference in the conditions of post-impact evolution. Therefore, the study of processes involved in impact cratering, or which result in impact craters at the moment of impact and subsequent transformation, as well as dating of these events, etc., is of utmost importance.

In such studies, a key role is played by the accessory mineral zircon (ZrSiO_4), which is capable of preserving information about processes occurring up to pressures of 80 GPa (e.g., [1,4,7,8]) due to the resistance of the mineral structure to high pressures, temperatures and chemical alteration, as well as its low capacity to incorporate trace elements into the structure during crystallization. While shock microstructures can be obscured in phases such as quartz, metamorphism following impact crater formation can be preserved in zircon (e.g., [5]). Zircon has been successfully used for dating young and ancient rocks using the U–Pb isotope system to obtain thermal history data on the basis of radiation dose calculation (e.g., [7,9]), as well as using the (U-Th)/He isotope system (e.g., [10]) and Ti content in zircon (e.g., [11]), and for determining the source of the lithology according to the trace element and isotope composition (e.g., [12–15]), etc.

The decay of radioactive impurities U and Th causes metamictization (amorphization) in zircon. This significant factor must be taken into account since it changes the properties of zircon and its durability (e.g., [9,16,17]). Micro-Raman spectroscopy is one of the most informative local quantitative methods for characterizing the metamict state (e.g., [9,16]). Raman spectra depend on the chemical composition, structure, interatomic bonds and degree of amorphization, as well as the orientation of the crystal lattice, etc. (e.g., [18]). This method is uniquely effective in terms of these measured local characteristics, low requirements for sample preparation (the surface of a solid material of any complexity, liquid and gaseous aggregate state of matter), as well as the high prevalence and availability of Raman devices in analytical labs. Among microbeam methods, micro-Raman spectroscopy is perhaps second only to optical and electron microscopy approaches, in terms of its effective use in earth sciences.

Raman spectroscopy is used for the following tasks in studies of the zircon [19,20]: identification of the mineral and high-pressure polymorphs (e.g., reidite, baddeleyite) [4,5,8,21–26]; diagnosing phase homogeneity [27]; characterization of the order/disorder state and measuring the degree of metamictization [28]; obtaining indirect data on the orientation and microstructural deformations of the crystal structure [29,30]; study of structural parameters and chemical bond characteristics (e.g., [31]); study of the phase transitions at different pressures and temperatures [32], semi-quantitative and quantitative measurement of the chemical composition based on empirical correlation of band parameters and composition of a solid solution (this is especially important for light elements and molecular groups) [33].

Moreover, attempts are being made to reveal Raman signatures of zircons of a certain genesis (asteroids, Mars, and Earth [34]), whether shocked or unshocked [4]. The authors of [4] showed that “Raman spectroscopy might be a useful tool for characterizing the shock stages of zircon crystals from natural and experimental impact environments”. However, the authors warned that the Raman spectra of shocked zircon may resemble those of metamict zircon, since the broadening and frequency shift of the Raman bands might also be due to strained zircon caused by shock waves or other sources of high-pressure-induced deformation or disorder in zircon.

The analysis of existing literature shows that zircons from impact craters are typically studied using electron backscatter diffraction (EBSD) in a scanning electron microscope (EBSD-SEM), and only a relatively small number of studies are based on Raman spectroscopy. There have also been a few attempts to investigate deformed zircon grains using Raman spectroscopy in combination with EBSD [23,29,30]. It has been demonstrated that shock deformations also affect the Raman spectra of zircon. Conversely, in studies of terrestrial zircons of non-impact origin, Raman is quite often used in comparison with EBSD [9–17,19,20,27,28]. Here, a discrepancy in the experience of the scientific groups using the different techniques can be noted. It is possible that progress in the study of impact zircons

is being hindered by an underestimation of the informational content and capabilities of Raman spectroscopy.

Thus, the aims of this review article are: (1) to determine the extent to which peer-reviewed scientific studies have applied Raman spectroscopy for investigating shocked zircon from terrestrial and lunar impactites over time; (2) to attract attention and encourage specialists to use the Raman spectroscopy method in the study of shocked zircons from impactites; (3) to highlight recent achievements and applications of Raman spectroscopy in this field.

2. Materials and Methods

A systematic literature review was carried out to identify data generated using Raman spectroscopy when studying shocked zircon grains in terrestrial and lunar impactites. Here, the major aim was to identify gaps in the use of Raman spectroscopy and propose the most effective applications. The review was produced in three steps: (1) a search for relevant studies; (2) selection of relevant studies; (3) analysis and synthesis of selected studies. For this systematic review, the PRISMA 2020 approach was used [35]. In accordance with this approach, a specialized flow diagram (Figure 1) and checklist (Supplementary Table S1) were completed.

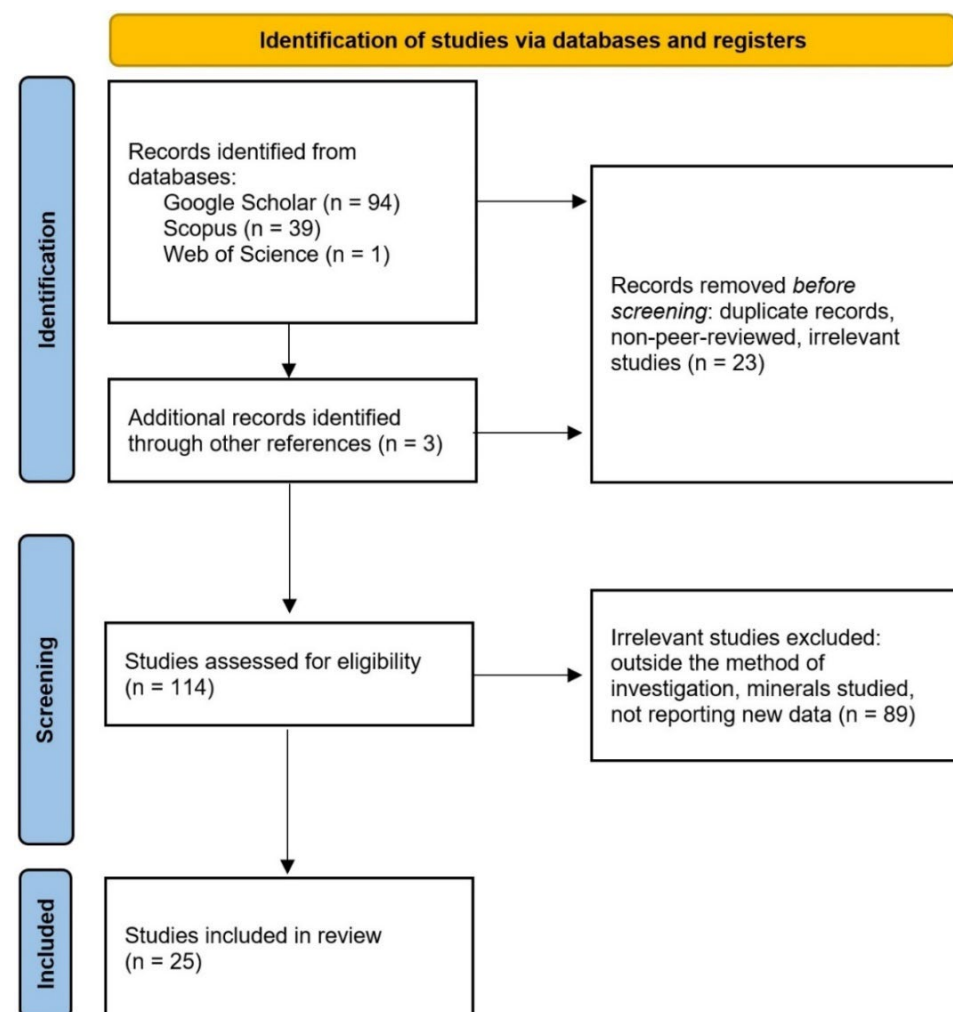


Figure 1. The systematic review protocol to obtain records for synthesis was conducted according to PRISMA guidelines, adapted from [35]. See PRISMA checklist in Supplementary Table S1. Combination of keywords *A* and *B* are shown below in Table 1. The search was carried out on 5 April 2022.

Table 1. Search strategy: number of hits on keywords and combined keywords in Google Scholar, Scopus, and Web of Science (Search: 5 April 2022).

Keywords	Google Scholar	Scopus	Web of Science
(1) "Raman"	3,220,000	1,392,577	383,538
(2) "Shocked zircon"	534	476	61
(3) "Impactites"	5420	1666	306
(4) "Lunar breccia"	2790	2285	54
Combined keywords			
A = (1) and (2) and (3)	83	26	1
B = (1) and (2) and (4)	11	13	0
Combinations A or B	94	39	1

2.1. Information Sources and Search Strategy

The search was based on Google Scholar, Scopus and Web of Science databases. Here, the studies of interest were those in which the method of Raman spectroscopy was applied to investigate natural zircon grains obtained from terrestrial and lunar geological impact structures that experienced a significant shock deformation. The material from extraterrestrial impactites was obtained through sampling during lunar missions or in the form of meteorites.

The eligibility criteria formulated for studies was set out as follows: "peer-reviewed studies in English language about the application of Raman spectroscopy to investigate shocked zircon obtained from natural terrestrial and lunar impactites". The keywords chosen were: (1) "Raman", (2) "shocked zircon", (3) "impactites", and (4) "lunar breccia" (Table 1). The set of keywords defined the method of investigation (1), the group of minerals (2), and the geological rocks (3, 4) in which they occur. Although results and conclusions were not included in the search criteria, an analysis of the results obtained in the papers is the subject of the "results" and "discussion" section of this work. In order to guarantee the eligibility criteria "application of Raman spectroscopy to investigate shocked zircon obtained from natural terrestrial and lunar impactites", two combinations of keywords $A = \{(1) \text{ and } (2) \text{ and } (3)\}$, $B = \{(1) \text{ and } (2) \text{ and } (4)\}$ were included in the search strategy (Table 1, Figure 1). From an examination of the bibliographies of the remaining papers and other sources, an additional 3 related studies were identified and scrutinized. The search was carried out on 5 April 2022.

2.2. The Process of Studies Selection, Inclusion and Exclusion Criteria

Microsoft Excel software was used to collage data reports and complete the first stage of the study selection. Search reports (combinations of keywords A and B) from databases (Scholar Google, Scopus, Web of Science) were imported via Excel worksheets. The sheet tables were filled by the listing of bibliographic citations in alphabetical sequence. To minimize the risk of bias, the search in the databases, and the data collection from each report, was independently performed twice.

To guarantee the robustness of the present review, only peer-reviewed studies in English were taken into consideration: comments and replies, conference abstracts, post-graduate dissertations and theses, and irrelevant book chapters were outside of the review's scope. To decide whether a study met this inclusion criterion, the database page devoted to each study or publisher page was read. The data on the studies were checked (peer-review, language, type of study) and markers were added in the document. After combining the data into a single worksheet, duplicated results were filtered, to result in 114 remaining unique results (Figure 1).

The studies were exported in free Mendeley desktop software [36] as reference list and PDF files, and metadata were downloaded automatically from the Mendeley online database. The completeness of all study metadata was checked and corrected by the author. To check the correspondence eligibility criteria, detailed analysis of the metadata

and full text reading of the studies was performed at the second stage of the study selection. Only studies that investigated terrestrial and lunar impactites were included for consideration in this review. The full texts were checked for the presence of keywords “Raman”, “shocked zircon”, “impactites” or “Lunar breccia”. Studies with keywords in the reference list and in context, but without new data, were removed. Three additional records were identified through additional references. Irrelevant studies of computer modelling, synthetic, experimentally shocked zircon, other minerals were excluded. Studies were marked as “include” or “exclude” in metadata tag fields. Thus, a total of 25 studies were selected for the present review (Table 2). Among the reviewed studies were 20 scientific articles and 5 book chapters.

Table 2. Results of the literature search (search: 5 April 2022). Studies are listed chronologically.

N	Publication Data (Bibliometric Parameters)			Microstructures in Zircon and Related Phases	Raman Data Presented			EBSD Data Presented	Application of Raman Data		
	Authors	Year	Publication		Spectra	Maps	Measured Band Parameters ¹		Phase Identification ²	Radiation Damage	Orientation Effect
1	Wopenka et al. [37]	1996	American Mineralogist	No data	yes	no	P, W	no	Zrn	no ³	no
2	Gucsik et al. [4]	2004	Cratering in Marine Environments and on Ice	Presence of reidite in zircon	yes	no	P	no	Rdt, Zrn	yes ⁴	no
3	Wittmann et al. [5]	2006	Meteoritics and Planetary Science	Granular texture, planar microstructure in zircon; reidite; ZrO ₂	yes	yes	P, W	no	Zrn, Rdt, ZrO ₂	yes ⁴	no
4	Gucsik [38]	2007	Acta Mineralogica Petrographica	Presence of reidite in zircon	yes	no	P	no	Rdt, Zrn	yes ⁴	no
5	Pati et al. [39]	2008	Meteoritics and Planetary Science	PFs, PDFs, granular texture	no	no	P	no	Zrn	no	no
6	Wittmann et al. [22]	2009	Geological Society of America Special Paper 458	Planar microstructures and granular texture in zircon; ZrO ₂	yes	no	P	no	Zrn, Bdl	no	no
7	Pidgeon et al. [40]	2011	Canadian Journal of Earth Sciences	Subparallel linear fractures	yes	no	P	no	Zrn	yes ⁴	no
8	Zhang et al. [41]	2011	Meteoritics and Planetary Science	Polycrystalline textures	yes	no	P	no	Zrn, ZrO ₂	no	no
9	Chen et al. [42]	2013	Meteoritics and Planetary Science	Lamellae reidite in zircon grain	yes	no	P	no	Rdt, Zrn	no	no
10	Grange et al. [43]	2013	Journal of Geophysical Research	Granular mixture of zircon and ZrO ₂	yes	no	No	no	Bdl, Zrn	no	no
11	Singleton et al. [7]	2015	Geological Society of America Special Paper 518	PF, granular texture, microporosity texture in zircon; reidite	yes	no	P	no	Zrn, Rdt	yes ⁴	no
12	Erickson et al. [23]	2017	Contributions to Mineralogy and Petrology	PDBs in zircon; lamellae and granular reidite;	yes	yes	P, W, R	yes	Rdt, Zrn	yes ⁵	no
13	Li et al. [44]	2018	Gondwana Research	PFs, PDFs in zircon; reidite	yes	no	P	no	Rdt, Zrn	no	no
14	McGregor et al. [45]	2018	Earth and Planetary Science Letters	PFs, granular textures in zircon	yes	no	P	no	Zrn	no	no
15	Pidgeon et al. [46]	2018	Meteoritics and Planetary Science	Non-planar fractures	yes	no	P, W	no	Zrn	yes ⁵	no
16	Kovaleva et al. [29]	2019	Geology	Granular texture	no	yes	P, W, R	yes	Zrn	yes ⁵	yes
17	Pati et al. [47]	2019	Meteoritics and Planetary Science	Granular texture in zircon; reidite	yes	no	P	yes	Rdt, Zrn	no	no
18	Walton et al. [48]	2019	Earth and Planetary Science Letters	Granular texture in zircon; reidite	yes	no	P	yes	Zrn, Rdt	no	no
19	Xing et al. [49]	2020	Geophysical Research Letters	Lamellar texture of reidite in zircon	yes	no	P	yes	Zrn, Rdt	no	no
20	Kaulina et al. [50]	2021	Geological and Geo-Environmental Processes on Earth	Presence of reidite in zircon	yes	no	P	yes	Rdt, Zrn	yes ⁴	no

21	Kovaleva and Zamyatin [30]	2021	Geological Society of America Special Paper 550	PDBs, microtwins, grain-size reduction	yes	yes	P, W, R	yes	Zrn	yes ⁵	yes
22	McGregor et al. [51]	2021	Contributions to Mineralogy and Petrology	Granular texture	yes	yes	P	yes	Zrn	yes ⁴	no
23	Wittmann et al. [52]	2021	Earth and Planetary Science Letters	Planar microstructures zircon; reidite lamellae	yes	no	P	yes	Zrn, Rdt	no ³	no
24	Huidobro et al. [53]	2021	ACS Earth and Space Chemistry	No data	yes	no	P	no	Zrn	no	no
25	Tartèse et al. [54]	2022	Meteoritics and Planetary Science	Presence of reidite in zircon	yes	no	P	no	Zrn	no ³	no

¹ P—position; W—width; R—intensity ratio of Raman bands. ² Zrn—zircon; Rdt—reidite. ³ Radiation dose calculated based on U, Th, Pb concentration; age by data isotope methods. ⁴ Radiation damage degree estimated qualitatively based on widening of zircon Raman bands. ⁵ Equivalent radiation dose $D_{\alpha^{eq}}$ estimated using FWHM Raman band $\nu_3(\text{SiO}_4)$.

2.3. Data Collection Process

Mendeley desktop was used to extract data from each study using the search option, by keywords (or their combination) along with analysis of abstracts and full texts. The data items extracted from studies were as follows: bibliometric parameters to characterize the level of research (authors, year, name of journal or book, quartile); geological objects and zircon microstructures to show how widely the Raman method was applied (terrestrial crater or lunar breccia, microstructures); Raman spectroscopy data presented in studies (spectra, maps, measured band parameters); application of Raman spectroscopy data to define what the method was used for (phase identification, radiation damage degree, orientation effects); EBSD data usage. These data were included in tabular form (Table 2) designed in accordance with the objectives of the review. The data items were ordered and presented in chronological sequence. Other variables for which data were sought included the journal quartile in SCImago, specialization of journals and books, methods, estimated pressures and temperatures.

To guarantee the robustness of the present review, only peer-reviewed studies published in English were considered. Abstracts were individually screened in order to exclude comments and replies, conference abstracts, postgraduate dissertations and theses, as well as irrelevant book chapters. After the filtration of duplicated papers, 114 unique studies remained (Figure 1) for which the full texts were then obtained. The reference list was exported using free Mendeley desktop software [36] in order to screen the abstracts and full text.

3. Results

The number of finds on keywords and combination of keywords in Google Scholar, Scopus, and Web of Science (searched on 5 April 2022) are presented on Table 1. The highest numbers of finds were through Google Scholar, while a significantly smaller number of articles resulted from the search using Scopus; fewer again were obtained using Web of Science. However, the analysis showed that more than half of the articles found through Google Scholar were not compliant with the eligibility criteria used for the review. Meanwhile, when using Web of Science, a significant number of included studies were lost. The closest number of matches was obtained from the Scopus database report.

The combination of keywords required the presence of each word to occur in the study. It can be observed from the table that the Raman method was a very commonly used term, but the objects of our study were less popular. There were very few studies of shocked zircons. Among the four keywords, the term “shocked zircon” was the narrowest criterion.

3.1. Objects and Specialization of Studies

Eighteen works examined terrestrial impact structures obtained from the following confirmed impact structure locations: Ries (Germany), Dhala (India), Chicxulub (Mexico), Popigai (Russia), Chesapeake Bay (U.S.A.), Haughton (Canada), Lac La Moine (Canada), Steen River (Canada), Nicholson Lake impact (Canada), Vredefort (South Africa) and Xiuyan (China), as well as potentially new terrestrial impact craters at Javrozzero and Järva-varaka (Kola–Karelian Region). Only four works performed a detailed study of lunar breccia samples obtained from Apollo missions 14, 15 and 17, and three works investigated NWA 11273, Sayh al Uhaymir 169 and Dhofar 458 lunar meteorites.

Book chapters were published in specialized books on the study of terrestrial impact craters, namely, *The ICDP-USGS Deep Drilling Project in the Chesapeake Bay impact structure: Results from the Eyreville Core Holes, Cratering in Marine Environments and on Ice*, and *Geological and Geo-Environmental Processes on Earth*, and proceedings of the homonymous international conference on all aspects of impact cratering and planetary science “Large Meteorite Impacts and Planetary Evolution V, VI”. Eleven papers (55% of the reviewed

studies published in journals) were published in specialized journals *Meteoritics and Planetary Science* [5,39,41,42,46,47,54], *Earth and Planetary Science Letters* [45,48,52], and *ACS Earth and Space Chemistry* [53]. Nine papers (45%) were presented in journals covering a wide scope of geology, mineralogy and petrology: *Geology* [29], *Gondwana Research* [43], *American Mineralogist* [37], *Canadian Journal of Earth Sciences* [40], *Contributions to Mineralogy and Petrology* [23,51], *Acta Mineralogica Petrographica* [38], *Journal of Geophysical Research* [43] and *Geophysical Research Letters* [49]. Nineteen papers were published in high-ranking journals of the first and second quartile (SCImago).

3.2. Microstructures in Zircon and Related Phases, Raman Spectroscopy Application

Zr-bearing phases were reported in reviewed studies (Table 2): zircon, reidite and ZrO_2 . The following microstructures in zircon and related phases were found: grain-size reduction, microtwins, granular texture, planar microstructures (planar fractures, planar deformation bands, planar deformation features), microporosity, lamellae reidite in zircon grains, granular reidite, ZrO_2 , granular mixture of zircon and ZrO_2 , curvilinear and non-planar fractures.

In all studies, the Raman peak position was presented, and phase identification was performed (Table 2). Raman spectra were not shown in [29,39] (8% of reviewed studies). Only five studies [5,23,29,30,51] used mapping to study zircon (20%). In 11 studies [2–5,7,23,29,30,38,40,46,50,51], Raman spectroscopy data were used to draw conclusions about the zircon radiation damage (44%). The radiation dose was calculated based on U, Th, and Pb concentration and ages using data isotope methods in three studies [37,52,54] (12%). Equivalent radiation dose D_{α}^{eq} was estimated using a full width at half-maximum (FWHM) Raman band ν_3 (SiO_4) in four studies [23,29,30,46] (16%). In seven studies [4,5,7,38,40,50,51], the degree of radiation damage was qualitatively estimated based on the widening of zircon Raman bands (28%). Only nine reviewed works [23,29,30,47–52] conducted investigations using the EBSD method (36%).

3.3. Main Results of Studies Found

According to the main results obtained, the reviewed studies could be roughly divided into two categories:

(1) Acquisition of new data and characterization of geological structures (nineteen studies): terrestrial impact craters [7,22,39,42,44,45,47,48,50–52,54] and lunar breccia [37,40,41,43,46,49,53]. These works were devoted to the dating of impact and post-impact events [39,41,43,44,49,51], the study of pressure–temperature paths at extreme conditions [7,22,42,45,47,48,52,54], obtaining data on radiation and thermal history [40,46], geochemical and mineralogical characterization [53], investigation of potentially new craters and identification of signs of impact processes [50]. In these 19 papers, Raman spectroscopy of zircon was recorded mainly to reveal polymorphic modifications and decomposition product of $ZrSiO_4$ (zircon, reidite, ZrO_2) by the presence of the corresponding Raman bands in spectra. The presence of polymorphs provided a fairly reliable indication of temperatures and pressures [1,2,8]. In some studies [7,22,37,46,50,51], the authors drew conclusions about the degree of zircon metamictization at a qualitative or quantitative level by band broadening or measuring the FWHM of the Raman band B_{1g} (1008 cm^{-1}), which is interpreted as asymmetric stretching of vibration mode ν_3 (SiO_4) [20,31,55];

(2) Investigation of different or specific deformations and identification of their textural or spectroscopic features (six studies): [4,5,23,29,30,38]. In these six papers, more detailed studies using Raman spectroscopy, its original applications, as well as the identification of Raman spectra in shocked zircons, were presented. The authors proposed to use Raman spectroscopy to diagnose the impact origin of zircons [4,5,23,38], to assess the degree of zircon metamictization [4,5,23,29,30], and reveal orientation effects [4,29,30,56].

The main results of the reviewed studies were briefly considered, to highlight the diversity of the outcomes of studies that used Raman spectroscopy (in chronological order, Table 2). Wopenka et al. [37] found that variations in the concentrations of U and Th

correlated strongly with those of other high-field-strength trace elements and with changes in Raman spectral parameters. Gucsik et al. [4] showed experimentally that shock damage of the zircon lattice resulted in broadening of the Raman spectral bands. Wittmann et al. [5] confirmed that shock deformation could cause amorphization of zircon crystal lattice. Gucsik et al. [38] concluded that Raman spectroscopy was a potentially useful tool that could be used to characterize the shock stage of zircons; a frequency shift of the 1000 cm^{-1} band was found in shocked zircon similar to that in radiation-damaged zircon. Pati et al. [39] confirmed the impact origin of the Dhala structure. Wittmann et al. [22] formed conclusions about temperature variations in the Chesapeake Bay crater. Pidgeon et al. [40] compared terrestrial and lunar shocked zircon grains. Examination of zircon samples did not reveal any grains with terrestrial-like shock features; most lunar zircons showed no evidence of a disturbance of their U–Pb systems. Zhang et al. [41] estimated that pressure $> 60\text{ GPa}$ and temperature $> 1700\text{ }^{\circ}\text{C}$ was achieved in lunar meteorite Dhofar 458; the U–Pb ages of impact event were measured. Chen et al. [42] studied the occurrence of reidite in the Xiuyan crater of China. Grange et al. [43] demonstrated that the U–Pb system of zircons indicated the age of resetting impact events; the pressure and temperature were estimated as $>60\text{ GPa}$ and $\sim 1700\text{ }^{\circ}\text{C}$. Singleton et al. [7] explored the effects of shock metamorphism on zircon from the Houghton impact structure (Canada); Raman spectroscopy data showed evidence of radiation damage, impurities, the presence of reidite, and recrystallized grains. Erickson et al. [23] studied zircon–reidite relationships to refine the impact conditions that produce this transformation, and quantified the geometric and crystallographic orientation relationships between these two phases. Li et al. [43] found that the REE patterns of zircon grains from structure Dhala were suggestive of a hydrothermal recrystallization in the presence of alkali-enriched fluids. McGregor et al. [45] applied in situ laser ablation inductively coupled plasma mass spectrometry (LA-ICP-MS) to obtain U–Pb ages, combined with the microstructural analysis of zircons; the authors proposed the use of relic phases as an alternative method for dating impact craters. Pidgeon et al. [46] demonstrated the unique value of zircon radiation damage ages in providing information on the thermal history and provenance of breccia samples from the Apollo 14 landing site. Kovaleva et al. [29] studied granular zircon from Vredefort granophyre (South Africa) and found radiation damage heterogeneity in individual neoblasts; the authors suggested that the host lithic clast was possibly captured near the top of the impact melt sheet and transported to the lowermost levels of the structure, traveling approximately 8–10 km. Pati et al. [47] provided a detailed look at shocked samples from the Dhala structure and reported on shatter cones, crystallographic indexing of planar deformation features, EBSD data for ballen quartz, and analysis of shocked zircon. Walton et al. [48] performed Raman spectroscopy and electron backscatter diffraction (EBSD) mapping, which confirmed the presence of reidite and coesite within some Steen River carbonate melt-bearing breccias. Xing et al. [49] discovered reidite in the regolith breccia of lunar meteorite Sayh al Uhaymir 169 and suggested that the reidite could have formed under localized transient pressure spikes during the initial stage of asteroid impact into porous lunar regolith. Kaulina et al. [50] studied potential astroblemes in the Kola–Korean region bearing signs of impact origin. Kovaleva and Zamyatin [30] used a combination of microbeam techniques to reveal the manifestation of deformation microstructure; they found that the ratio B_{1g}/E_g of Raman band intensity maps combined with metamictization degree maps was sensitive to shock deformation features in zircon. McGregor et al. [51] provided a microstructural framework outlining the sequential evolution of zircon, titanite, and apatite during shock and thermal metamorphism. Wittmann et al. [52] revealed a statistically significant correlation of the occurrence of planar fractures in zircon with the types of host materials, and suggested amplification of pressure due to shock impedance contrasts between zircon and its mineral hosts. Huidobro et al. [53] analyzed a lunar feldspathic breccia meteorite NWA 11273 to compensate for the lack of scientific data available about its mineralogy and geochemistry. Tartèse et al. [54] studied zircon

and monazite from the uplifted Variscan crystalline basement of the Ries impact crater, produced U–Pb dating and did not confirm reidite presence by Raman spectroscopy.

A non-systematic primary review of the literature showed that Raman spectroscopy was applied to impact terrestrial rocks, and that the Raman method was even more limited for meteorites and lunar rocks due to the small grain size of zircons. The presence of deformations in zircon grains is rare and irregular in meteorites, and a small number of high-pressure polymorphs has been discovered in lunar samples [34].

4. Discussion

This section discusses the application of Raman spectroscopy to certain aspects of the study of shocked zircons from impactites, highlighting advantages, working and promising applications, and formulating some recommendations on the use of the equipment.

4.1. Increase in the Number of Studies

Of the 25 identified studies, the earliest publication [37] investigated a single zoned zircon grain in a thin section of a 23 mg lithic fragment, comprising lunar samples 14, 161 and 7069 obtained from an Apollo 14 soil (Table 2). The next study was a chapter in the book *Cratering in Marine Environments and on Ice* [4], which studied cathodoluminescence, electron microscopy, and Raman spectroscopy of experimentally and naturally shocked zircon crystals. This investigation set out to understand the capability of SEM-CL and Raman techniques to determine whether specific CL or Raman effects in zircon/scheelite-structure can be used to determine particular shock pressure stages. The next published paper was “Shock-metamorphosed zircon in terrestrial impact craters” [5]. Here the authors compared zircon grains from Ries, Popigai and Chicxulub impact craters, which were subjected to pressures of up to 80 GPa. Since 2006, papers in which Raman spectroscopy was used to study zircons in terrestrial and extraterrestrial impacts have been published every year (Figure 2). The maximum number of studies published annually was five (2021).

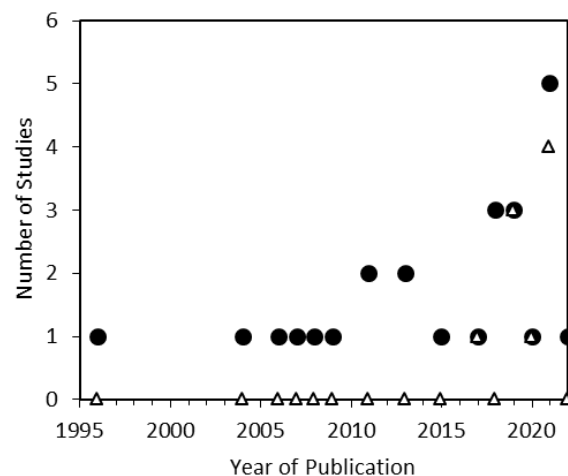


Figure 2. Number of reviewed studies per year (filled cycle), and number of reviewed studies where Raman and SEM-EBSD methods were used (open triangle). The search was carried out on 5 April 2022.

The history of the application of Raman spectroscopy to the investigation of impactite zircons is linked with the development of Raman spectroscopy in studying zircons from various rocks and origin. A search for the keywords “Raman” and “zircon” in the Scopus database showed that one of the first published texts containing these words dates back to 1969 [57]. After that, there were regular studies in the amount of less than 20 per year until 1994. Since 1996, their number has doubled; since 2005, the number of studies per year has not fallen below 100. In 2021, a peak value of 767 studies was observed. One of

the triggers for the dramatic increase in studies was the progress in applying Raman spectroscopy to the study of zircon samples that had been fully or partially amorphized due to radioactivity [28] and the establishment of quantitative correlations between Raman band parameters and the degree of radiation damage (metamictization) [9,16,28,58].

Another important factor in the growth of shocked zircon studies was the development of the EBSD technique in the early 2000s. Before 2017, the zirconology of impactites was developing in the fields of deformation analysis, U–Pb-dating and the study of U–Pb-isotope system behavior as a response to various impact pressures and temperatures (e.g., [59,60]). The first publication of Raman spectra in a scientific article [23] occurred only in 2017, where Raman spectra were presented for a qualitative characterization of the degree of zircon metamict together with analysis of microstructural deformations in shocked zircons according to EBSD data. Since then, the number of studies reporting EBSD and Raman spectroscopy data together has begun to increase (Figure 2). Nevertheless, it should be noted that, even today, specialists in deformation zirconology pay scant attention to the Raman spectroscopy method. According to the Scopus database, 141 articles were published in 2021 in which the words “zircon” and “EBSD” appear, of which only four reported the Raman spectra of zircons (Figure 2). This would seem to imply a narrowly utilitarian use solely for assessing the degree of metamictization and identifying polymorphs. The unpopularity of the method is probably either due to the EBSD method allowing researchers to obtain the necessary data without involving the application of Raman spectroscopy, or to an underestimation of the possibilities of the Raman method.

4.2. Radiation Damage Degree and Raman Spectroscopy Signatures of Shocked Zircon

Zircon of any origin experiences radiation damage due to radioactive decay of U and Th elements incorporated during growth and secondary alteration processes (e.g., [17,61,62]). Different U and Th concentrations in zircon zones (domains) and complicated thermal annealing histories lead to various extents of radiation damage in zircon zones, which can be easily detected in grains using CL and BSE images (e.g., [61,63]). The most reliable and well developed microbeam method for measuring the degree of radiation damage in zircon zones is Raman spectroscopy [20,33]. The increase in radiation dose shifts and widens the Raman bands, leading to a decrease in their intensity (Figure 3).

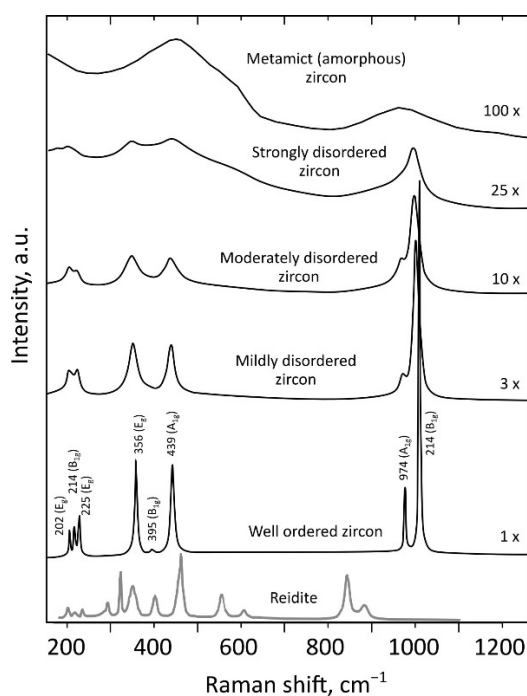


Figure 3. Raman spectra in zircon with various degrees of radiation damage (structure disorder) and high-pressure polymorph reidite. Modified after [9,56].

The correlation of FWHM of Raman band $\nu_3(\text{SiO}_4)$ at $\sim 1008 \text{ cm}^{-1}$ with radiation dose (Figure 4) in natural zircons is well studied [9,16,28,58]. It allows the measurement of the radiation damage degree and the study of the thermal history [9,10,28,46,64]. Equivalent dose $D_{\alpha^{\text{ed}}}$ could be measured using a developed equation (e.g., [40,65]) taking the FWHM of $\nu_3(\text{SiO}_4)$. The data on U and Th concentrations in spots measured by laser ablation inductively coupled plasma mass spectrometry (LA-ICP-MS), electron probe microanalysis (EPMA), or secondary ion mass spectrometry (SIMS), could be used to calculate accumulated (time-integrated) radiation dose D_{α} in accordance with [66,67].

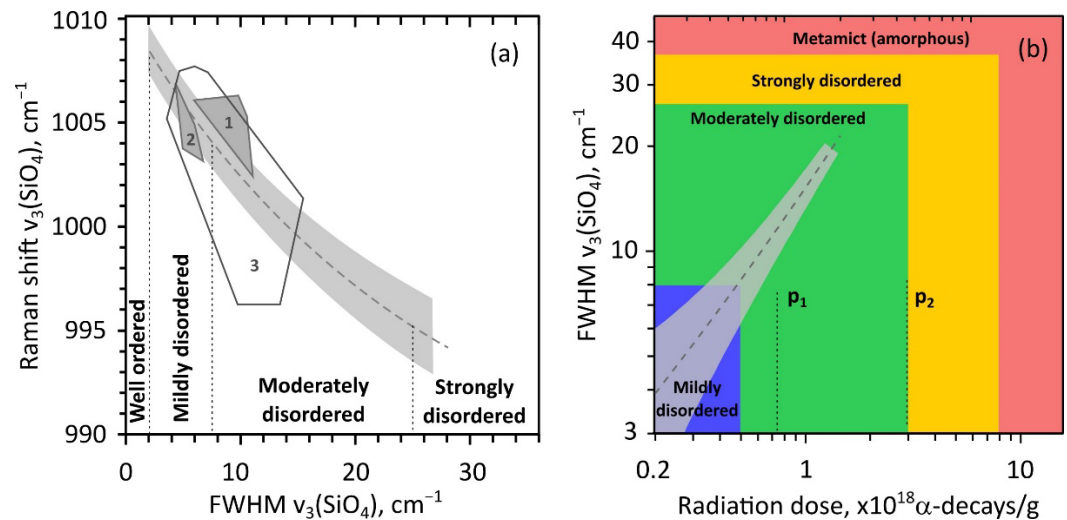


Figure 4. Raman band parameters and radiation doses: (a) Raman shift and FWHM (full width at half maximum) of band $\nu_3(\text{SiO}_4)$ polygons were built using the data of [5] (dark-gray field 1 is Reis, dark-gray field 2 is Popigai, dark-gray solid line 3 is Chicxulub crater, dotted line is boundaries between levels of structure disorder); (b) Plot of FWHM $\nu_3(\text{SiO}_4)$ against the equivalent radiation dose $D_{\alpha^{\text{ed}}}$; the positions of percolation points p_1 , p_2 [68,69] and the boundaries between levels of structure disorder (colors) are debatable and shown approximately. The light gray fields with broken lines (in (a,b)) are regions of calibrated values on natural unaltered and unstressed samples, according to [9].

The time needed to generate the observed radiation damage is referred to as the radiation damage age. The dating of geological events of significant thermal heating can be roughly used as an approximation to radiation damage age in the equations [45]. Using the value of $D_{\alpha^{\text{ed}}}$ or FWHM $\nu_3(\text{SiO}_4)$, the metamictization degree of zircon can be classified (Figure 4b), while the edges between stages of structure disorder are not strictly defined [66,67,70]: well-ordered ($D_{\alpha^{\text{ed}}} < 0.2 \cdot 10^{18} \alpha\text{-decays/g}$; $\text{FWHM } \nu_3(\text{SiO}_4) < 2 \text{ cm}^{-1}$); mildly damaged ($0.2 \cdot 10^{18} < D_{\alpha^{\text{ed}}} < 0.5 \cdot 10^{18}$; $2 < \text{FWHM} < 8$); moderately damaged ($0.5 \cdot 10^{18} < D_{\alpha^{\text{ed}}} < 2 \cdot 10^{18}$; $8 < \text{FWHM} < 25$); strongly damaged ($2 \cdot 10^{18} < D_{\alpha^{\text{ed}}} < 8 \cdot 10^{18}$; $25 < \text{FWHM} < 35$); or metamict ($D_{\alpha^{\text{ed}}} > 8 \cdot 10^{18}$; $\text{FWHM} > 35$). The first and second percolation points (critical points in changing properties with an increase in the degree of radiation damage) p_1 and p_2 , correspond approximately to doses of $0.75 \cdot 10^{18}$ and $3 \cdot 10^{18} \alpha\text{-decays/g}$ [68,69].

Since the ratio of Raman band intensities in zircon is sensitive to radiation damage, the degree and mapping of the band ratio can be used to reveal the distribution of damage [23]. Additional orientation effect on band ratios could also be significant [29,30]. Hence, it is preferable to reveal the damage by mapping the Raman band width. The Raman band $\nu_3(\text{SiO}_4)$ FWHM was measured in reviewed papers [5,23,29,30,40,50]. The equivalent or accumulated radiation doses were calculated in [23,29,37,40,51]. Conclusions about the radiation annealing history were drawn in [29,37,40,51].

Wittmann et al. [4] found that Raman spectra showed variable intensity ratios of the $\nu_3(\text{SiO}_4)$ Raman bands of zircon that spanned a range of frequencies and FWHM, that were in accordance with the amorphization trends of relic zircon domains in

experimentally shocked ZrSiO_4 [4]. Erickson et al. [23] showed, using Raman spectroscopy mapping, that moderate metamictization could inhibit reidite formation, thereby highlighting that the transformation was controlled by zircon crystallinity. The mapping of the ratio of $\nu_3(\text{SiO}_4)$ to the $\nu_1(\text{SiO}_4)$ peak was sensitive to short-range order of the crystal structure, and thus was a proxy for metamictization. The authors of [40] concluded that the Raman spectra of zircon grains consisted of the typical zircon peaks and showed a broadening of the bands with increasing U content of the zircon; there was no evidence in the Raman spectra for a component of damage that could be attributed to shock as reported by [4]. It was highlighted in [50] that zircon cores were mainly represented by crystalline domains with moderate to strong degree of metamictization, while the total absence of peaks in the spectrum of rims could indicate amorphization of the crystal lattice.

The crystallinity of zircon at the moment of meteorite impact determines the transformation to reidite among other factors [5,23,71]. Erickson et al. [23] highlighted that “Although moderately metamict zircon will hinder the development of lamellar reidite during shock metamorphism, granular reidite will preferentially nucleate in zircon domains with high levels of amorphization.” These peculiarities distinguish shocked zircons from their non-shocked equivalents. The degree of radiation damage of zircon grains from meteorites is also at the stage of detailed study [34]. Roszjar et al. [34] measured FWHM and $\nu_3(\text{SiO}_4)$ band position in zircon to indicate a certain degree of radiation damage and structural annealing observed in grains. The authors suggested that a subset of zircon from meteorites grains showed an unusual downshift in the position of the band, compared with terrestrial grains. Hence, the calculation of the radiation damage degree at the moment of impact and the study of the annealing history are of particular importance for impactite zircons.

Gucsik et al. [72,73] performed the first systematic CL and Raman studies of shocked zircon grains from nature and laboratory shock experiments. Gucsik et al. [4] reported an increase in the width of Raman band $\nu_3(\text{SiO}_4)$ in experimentally shocked natural zircon at a shock pressure of 20 GPa. The authors noted that “this observation could imply a possible similar defective crystal structure between the (radiation) damaged and shocked zircon” and that “frequency shifts of the 1000 cm^{-1} band by a few cm^{-1} might be due to strained zircon caused by shock waves or high-pressure-induced deformation or disorder in zircon. Similar frequency shifts were observed in radiation-damaged zircon.” The change in the position and width of the $\nu_3(\text{SiO}_4)$ band was explained in terms of pressure-induced deformation, local defects and strain. The different values of these parameters in the sample confirmed the heterogeneity of the shock pressure. Gucsik et al. [73] concluded that Raman spectra provided a potential means to estimate shock pressure across the bandwidth. The authors considered that changes in position and width of Raman bands were most likely associated with defects, which made the application of these parameters more difficult. In further studies of natural zircons, no evidence in the Raman spectra was observed for a component of damage that could be definitely attributed to shock (e.g., [5,7,29,30,50]). The majority of Raman band shifts to low wavenumbers fell within the range of error for the peak assignment (Figure 4), which was very similar to those representing damage induced by radiation [7,29,30,50]. Further detailed studies of the metamict state caused by shock deformation are necessary; the effect should be taken into account when interpreting the amorphization causes of shocked zircon and in understanding the annealing history. To date, the only reliable Raman spectrum marker that could be considered as unique for shocked zircon is the presence of Raman bands of high-pressure polymorphs reidite and ZrO_2 [4,5,8,21–25,73,74]. Nonetheless, the combination of BSE and CL imaging with CL and Raman spectroscopy is a potentially useful tool that can be used to characterize the shock stage of zircons obtained from impactites. The authors of [72,73] found that shocked zircon could be a powerful tool for the shock stage determination of shocked minerals using Raman and CL spectroscopy.

4.3. Orientation Effect and Microstructural Deformations

The following zircon microstructural impact-related features were reported in the reviewed studies (Table 2): planar fractures, planar deformation bands, planar deformation features, granular texture, micro-porosity texture, zircon micro-twin lamellae, reidite lamellae, zircon decomposition to ZrO_2 . The authors identified these diverse textural features as having arisen at various pressures up to 80 GPa, and temperatures up to 1700 °C (Table 2); textural features of micro-deformations were studied by optical microscope and EBSD.

The authors of [29,30] applied Raman spectroscopy to distinguish textural features (PDBs, microtwins, subgrains and granular zircon) in shocked zircon. The intensity of Raman bands is not only sensitive to the crystal orientation of zircon, but also to other factors (chemical composition, radiation damage degree, presence of other phases, etc.), which presents challenges when applying Raman band intensities to quantitative analysis. In the majority of terrestrial zircons that do not have microstructural deformation, the Raman map by band intensity repeats the texture that appears in the Raman map by band width that shows zircon zones with varying degrees of metamictization. The same textures are revealed on BSE and CL images [19,23,29,30] and Raman maps by band position, in which additional strain appears along the fractures. Nevertheless, mapping of the Raman band intensity ratios can be effectively used to identify and visualize inhomogeneities in the crystal lattice orientation.

The authors of [29] used the ratio of Raman band intensities B_{1g} (1008 cm^{-1}) to E_g (356 cm^{-1}) to distinguish crystal lattice misorientation in granular shocked zircon. The Raman B_{1g}/E_g band intensity ratio map reveals a patchy signal (Figure 5d), which is different from the systematic variations of FWHM B_{1g} caused by the degree of metamictization (Figure 5e). Notably, orientation of domains (region A and B) in the EBSD inverse pole figure map (Figure 5a) and in the Raman B_{1g}/E_g intensity ratio map (Figure 5d) are roughly correlated. Thus, the heterogeneity in the B_{1g}/E_g ratio can be attributed to variations of crystal orientation, but not to metamictization. The same effect was studied in tectonically deformed, seismically deformed, and shocked zircon grains [30]. Here, the authors found that the B_{1g}/E_g ratio was affected in shocked zircons, particularly in twinned domains with high misorientation.

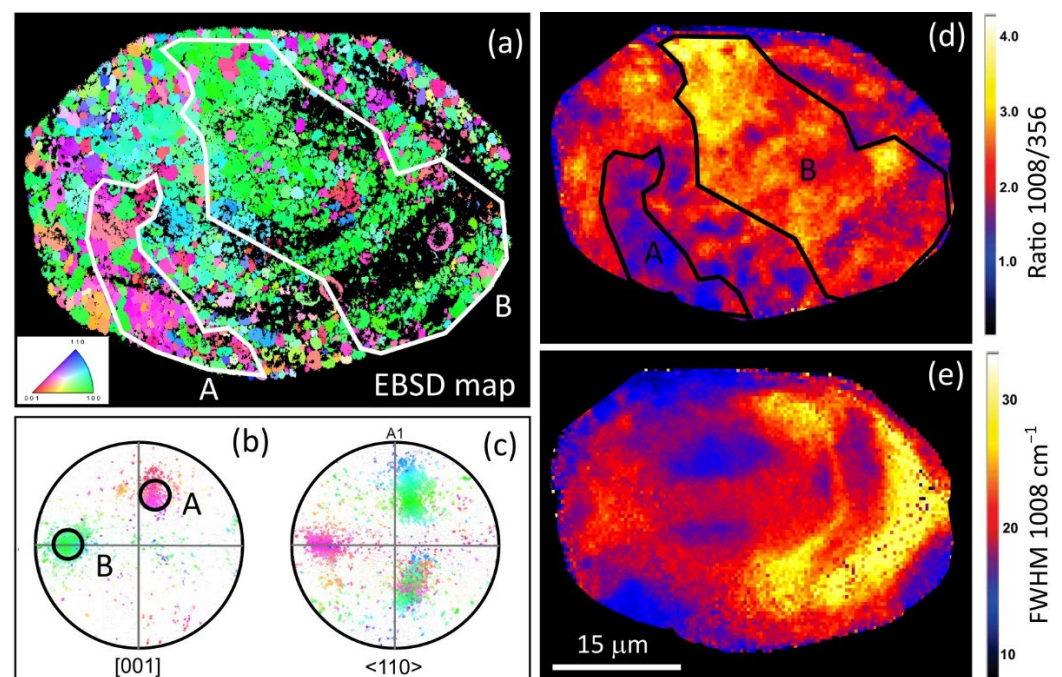


Figure 5. Correlation of EBSD and Raman spectroscopy data: (a) EBSD orientation inverse pole figure map, showing two major orientation groups: pink–orange (A), and green–blue (B); (b,c) equal

angle lower hemisphere projection pole figures for zircon [001] and $\langle 110 \rangle$ directions, color coded as in (a); (d) Raman band intensity ratio B_{1g}/E_g map shows patchy distribution (E_g is a Raman band at 356 cm^{-1} , B_{1g} is a band at 1008 cm^{-1}); (e) full width at half maximum (FWHM) of Raman band B_{1g} (1008 cm^{-1}) shows spatial variations in degree of radiation damage. Modified after [29]. Orientational groups of domains are marked as regions A and B.

Thus, the difference in texture manifested by B_{1g}/E_g ratio mapping and metamictization degree maps (FWHM of B_{1g} band or alternatively CL image) is a new signature of shock deformation features in zircon, which could be used as Raman spectroscopy marker of shocked zircon. Here, it is necessary to take into account that the variations in peak intensity ratios in zircon grain depend on orientation with respect to the polarization plane of the laser beam. Prospects for the practical use of this effect are limited by the lower spatial resolution of Raman spectroscopy in comparison with the EBSD technique.

At the present time, the use of Raman spectroscopy for orientation analysis only allows the diagnosis of high angle misorientations. Moreover, analysis of spectra in spots is insufficient; hypermapping is significantly more informative. Analysis of several Raman maps having different orientations of the polarization plane of the laser beam with respect to the grain, along with the use of a polarizer, can significantly improve the accuracy of misorientation diagnostics. It is anticipated that a polarizer can be used to determine the relative orientation of the fragments. However, this is unlikely to obtain more accurate data than the EBSD method.

4.4. Identification of Zircon Polymorphs and Products of Its Decomposition

Zircon responds to shock metamorphism in various ways: crystal-plasticity, twinning, transformation to reidite, formation of granular texture, and decomposition to polymorphs zirconia (ZrO_2) and silica (SiO_2). The resulting textural features consisting of $ZrSiO_4$, ZrO_2 and SiO_2 polymorphs provide robust thermobarometers that record different extreme conditions [8]. Extreme conditions induce transformation of zircon to reidite at pressures $> 38\text{ GPa}$ (e.g., [4,5,21–23,75]), as well as decomposition to ZrO_2 and SiO_2 polymorphs at $T > 1673\text{ }^\circ\text{C}$ (e.g., [5,8,22,24,25,73,74]). Depending on the P–T-path and other factors (chemical composition, surrounding minerals, metamict state), SiO_2 can be presented as cubic (β -cristobalite), trigonal (α -quartz), hexagonal (β -quartz, β -tridymite), orthorhombic (α -tridymite), tetragonal (α -cristobalite or stishovite), monoclinic (coesite, tridymite) or amorphous silica glass (lechatelierite), while ZrO_2 can be presented as monoclinic (baddeleyite, m- ZrO_2), cubic (c- ZrO_2), tetragonal (t- ZrO_2) or orthorhombic (oI- ZrO_2 or oII- ZrO_2) polymorphs. Polymorphs of Zr-bearing high-pressure and high-temperature phases have been found in terrestrial [7,22,23,38,42,44,46–48,50,52] and lunar [43] impactites, as well as in lunar meteorites (e.g., the first discovered reidite in the regolith portion of the Sayh al Uhaymir lunar meteorite [49]).

The well-known Raman spectra of $ZrSiO_4$, ZrO_2 and SiO_2 polymorphs are composed of a number of narrow and wide bands (Figures 3 and 6). However, determining the polymorphs of the mixture may be impossible due to the presence of several phases [4,5,22,50]. The exact band location and intensity may be affected by a number of factors, including degree of crystallinity (Figure 3), integration of nonformula elements, nearby phases, and radiation damage [20,76,77]. A better phase search can be achieved by increasing the spectral resolution of the equipment. To do this, it is necessary to choose an energy range with higher spectral resolution on equipment having a long path monochromator (at least 800 mm) and diffraction gratings with a high line density (at least 1800 g/mm). A triple configuration Raman spectrometer (Horiba T64000) has the best spectral resolution. However, no equipment can produce narrow Raman bands that are wide by nature.

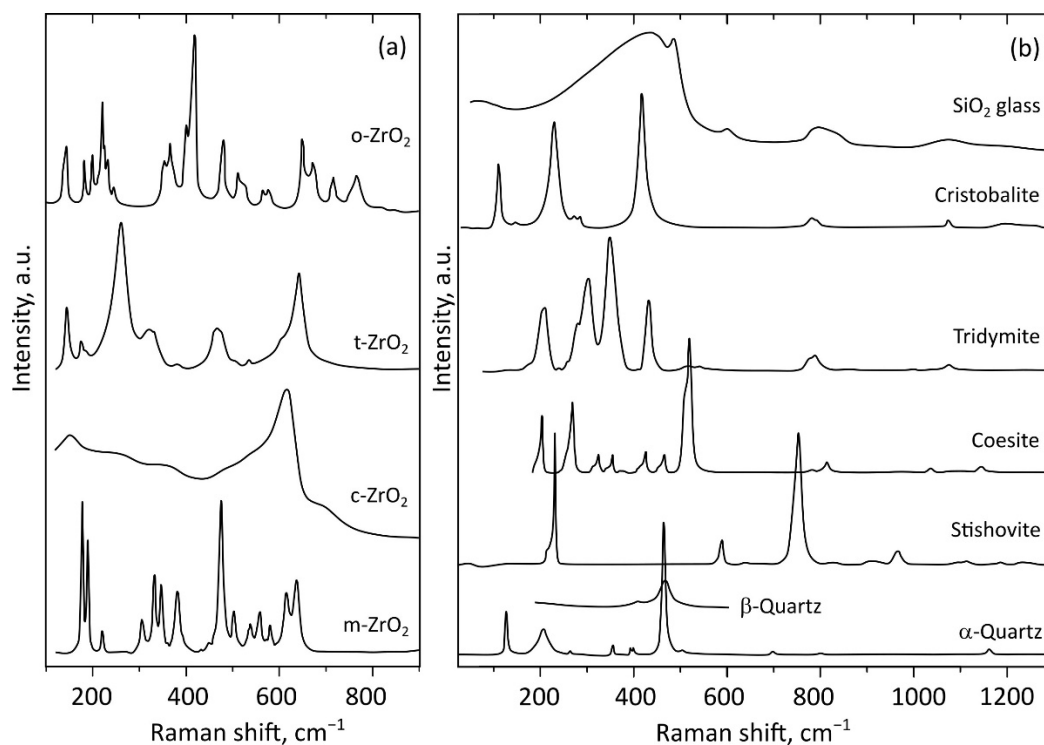


Figure 6. Raman spectra of ZrO₂ (a), and SiO₂ (b), polymorphs. Modified after [76,77].

Polymorphs typically appear in zircon grains as textural features of a few micrometers or less in size, descending to a few nanometers. Gucsik et al. [72,73] performed the first systematic CL and Raman spectroscopy studies of the shocked zircon grains from nature and experiment. The Raman spectra of the unshocked and experimentally shocked samples at 20, 40, and 60 GPa pressures were distinctly different. The 40 and 60 GPa samples demonstrated the presence of a reidite phase. The authors considered that the different Raman band intensities of zircon and reidite phases along the sample reflected the heterogeneity of the shock pressure, while the intensity ratio reflected the relative contents of the two phases. The presence of both phases in Raman spectra indicates that the untransformed zircon remnants are smaller than the laser beam size (~1 mm).

In comparison with EBSD, which allows registration at the level of tens of nanometers, the spatial resolution is the main factor limiting the application of Raman spectroscopy. The actual lateral and depth resolutions of Raman spectroscopy depend on surface roughness, refraction, and many other factors [19]. The usage of a confocal optical system equipped with a $\times 100$ lens offering a high numerical aperture (NA) value, laser excitation lines with a short wavelength (e.g., 473, 488 nm) and small size of the entrance hole of monochromator ($< 50 \mu\text{m}$) allows lateral and depth spatial resolution to be increased to below $\sim 1 \mu\text{m}$. Even at this resolution, however, EBSD maps resolve significantly more details, compared with Raman maps of micrometer phases. Nevertheless, in the case of nano-sized mixtures, the EBSD method demonstrates smoothed low quality Kikuchi patterns, which often do not allow the detection of phases in grains. In contrast, while the spatial resolution of Raman technique is $\sim 1 \mu\text{m}$, its spectra usually contain components of even nano-sized mixture phases (e.g., [3,23]). The different nature of Raman spectroscopy and EBSD approaches inspire the combined usage of both techniques to study polymorph mineral phases in shocked zircon, depending on the phase's size. In particular, the Raman technique offers advantages when studying nano-sized mixtures.

ZrSiO₄, SiO₂, ZrO₂ phases have a limited capacity to absorb trace elements. This means that the corresponding Raman band parameters do not depend significantly on the concentration of trace elements. Although peak positions and widths are potentially more

sensitive to structural peculiarities and interatomic bonds arising due to zircon shock modification, this issue has not been studied in detail.

For registration of correct spectra, it is important to perform a meticulous choice of the laser line excitation. Laser lines 633, 532, 514, 488 and 473 nm are the most accessible and widely used. Powerful blue laser lines can induce heating or transformation under the laser beam. The laser lines 514 and 532 nm excite thin photoluminescent peaks of REE in the range of main Si–O vibrations. These peaks can be misinterpreted as Raman bands of zircon polymorph or product of decomposition (phases of ZrO_2 and SiO_2). Since the red line 633 nm is free of these disadvantages, it is the most preferable for recording zircon Raman spectra.

4.5. The Advantages of Zircon in the Impact Studies

Publications that were relevant to the subject under consideration but did not meet the eligibility criteria for the systematic review were also briefly considered. The main types of shock effects are associated with increasing shock pressure: mechanical deformations, phase transformations, decomposition, and/or melting. Common rock-forming minerals, such as quartz, plagioclase, alkali feldspar, olivine, pyroxene, amphibole, biotite, differ in terms of the range of these effects and demonstrate shock mosaicism, planar deformation features, diaplectic glass formation, kink bands or twins [1]. In addition, accessory minerals such as garnet, sillimanite, cordierite, zircon, ilmenite, Fe-sulfides, magnetite, graphite, etc., also display shock effects. The advantages of zircon in comparison with other minerals are as follows: it occurs in almost all target rocks; it is capable of preserving information about processes occurring up to pressures of 80 GPa [1,4,7,8]; and it is resistant to secondary alteration process and preserves deformation microstructures [8]. Dislocations in zircon form at pressures below 20 GPa, planar deformations bands form at pressure of 5–25 GPa, microtwins form at pressure of 20–35 GPa, transition to reidite occurs at >30 GPa, and decomposition into ZrO_2 and SiO_2 at post-shock temperatures above 1670 °C [1,8]. It should be noted that microtwins do not form in zircon under pressures below 13 GPa. In this range, it is possible to determine achieved pressures more accurately using other minerals, such as titanite [78]. While consideration of several mineral systems is preferable, it is not always possible.

An indisputable advantage of zircon over other minerals when used in impact studies is its wide use for U–Pb dating. The U–Pb system in zircon has a higher closure temperature in comparison with other minerals (apatite, baddeleyite, monazite, xenotime, and titanite, e.g., [79]) and a longer decay time compared with other isotope systems. Zircon is a robust, refractory mineral that is isotopically resistant to post-impact thermal overprinting, but shock metamorphism could reset the U–Pb content of zircon. These features allow both the original age of the target rocks and the time of isotopic resetting to be recorded even in large ancient terrestrial impact craters and lunar breccia. Kamo et al. [79] noted “Thus, it would appear... that Pb loss in zircon is predominantly controlled by the intensity of impact-induced shock metamorphism.” This conclusion is confirmed by other studies [41,43,80–85]. The U–Pb system continues to be preserved at high pressures and temperatures when other minerals might already have been melted down or altered, disturbing the isotope systems. Zircon plays a key role, not only in the age determination of the terrestrial impact structures [51,59,60,80,81], but also the lunar breccia and meteorites [37,41,43,46,86]. All these features of zircon make it an outstanding mineral for studying impact structures.

5. Conclusions

The current study presented a systematic literature review aimed at determining the extent to which peer-reviewed scientific studies have applied Raman spectroscopy for investigating shocked zircon from terrestrial and lunar impactites over time, as well as highlighting recent achievements and the most effective applications of the Raman method. A total of 25 research studies were selected for the present review. Among these studies

were 20 scientific articles and 5 book chapters. Terrestrial impact structures were studied in 18 papers, while only 4 studies investigated lunar breccia samples and 3 were devoted to lunar meteorites. The reviewed studies were divided into two categories: (1) acquisition of new data and characterization of geological structures (19 studies); and, (2) investigation of different microstructural deformations and identification of their textural or spectroscopic features (six studies).

The history of the application of Raman spectroscopy in the investigation of impactite zircons is inextricably linked with the development of Raman spectroscopy as a means of investigating zircons of various terrestrial rocks, as well as the development of the EBSD technique during the early 2000s. The number of studies reporting both EBSD and Raman spectroscopy data has started to expand since 2017. However, even today, specialists in zirconology investigating deformations pay only scant attention to the Raman spectroscopy method. The unpopularity of the method is probably either due to the EBSD method allowing researchers to obtain the necessary data without involving the application of Raman spectroscopy, or to an underestimation of the possibilities of the Raman method.

The main applications and capabilities of the Raman method in the study of shocked zircon, as well as its advantages over the more commonly used EBSD approach, were highlighted in this review:

- (1) The degree of radiation damage at the moment of impact and the annealing history are of particular importance when studying impactite zircons. When interpreting the reasons for amorphization of shocked zircon and attempting to understand the annealing history, the effect of widening Raman bands due to deformation should be taken into account. For this, it is necessary to calculate and measure the degree of damage using Raman spectra;
- (2) Mapping of the Raman band intensity ratios can be effectively used to identify and visualize inhomogeneities in the crystal lattice orientation. Thus, the Raman band ratio of B_{1g}/E_g and degree of metamictization maps combined is a signature of shock deformation features in zircon, which can be used as Raman spectroscopy marker of shocked zircon;
- (3) In the case of nano-sized phase mixtures, the EBSD method demonstrates smoothed low quality Kikuchi patterns, which often create problems in the detection of polymorph phases. In contrast, Raman spectra typically contain components of even nano-sized mixed phases. The different nature of Raman spectroscopy and EBSD methods motivate the combined usage of both techniques to study polymorph mineral phases in zircon, depending on the size of the phase. The most reliable Raman spectrum marker, which could be considered as unique for shocked zircon, is the presence of Raman bands of high-pressure polymorph reidite and orthorhombic ZrO_2 ;
- (4) The high availability, registration speed and low sample preparation requirements of Raman spectrometers lowers the threshold to start studies on rocks obtained from impact craters.

The main disadvantage of the Raman method is the low spatial resolution in comparison with EBSD (registration at the level of tens of nanometers) and low sensitivity to the orientation of the crystal lattice.

The above indicates that the Raman spectroscopy method cannot replace EBSD. Rather, Raman spectroscopy comprises an independent sensitive search method for polymorphs obtaining unique data and preliminary data on misorientations. It is convenient to first conduct an investigation on a Raman spectrometer, and then analyze the grains in more detail using EBSD, to obtain data on the orientation of the grains. In this systematic review, the capabilities of Raman spectroscopy have been highlighted. It is hoped that this will initiate future progress in the investigation of impact zircons.

Supplementary Materials: The following supporting information can be downloaded at: <https://www.mdpi.com/article/10.3390/min12080969/s1>, Table S1: PRISMA 2020 checklist.

Funding: This work was supported by the Russian Science Foundation: 21-77-10019; Ministry of Science and Higher Education of Russian Federation: 075-15-2021-680.

Data Availability Statement: Not applicable.

Acknowledgments: The author is grateful to Elizaveta Kovaleva for the idea to prepare a review article, as well as for subsequent consultations and discussions.

Conflicts of Interest: The author declares no conflict of interest. The funders had no role in the design of the study; in the collection, analyses, or interpretation of data; in the writing of the manuscript, or in the decision to publish the results.

References

1. Stöffler, D.; Hamann, C.; Metzler, K. Shock metamorphism of planetary silicate rocks and sediments: Proposal for an updated classification system. *Meteorit. Planet. Sci.* **2018**, *53*, 5–49. <https://doi.org/10.1111/maps.12912>.
2. Melosh, H.L. *Impact Cratering: A Geological Process*; Oxford University Press: New York, NY, USA, 1989.
3. Leroux, H.; Reimold, W.U.; Koeberl, C.; Hornemann, U.; Doukhan, J.C. Experimental shock deformation in zircon: A transmission electron microscopic study. *Earth Planet. Sci. Lett.* **1999**, *169*, 291–301. [https://doi.org/10.1016/S0012-821X\(99\)00082-5](https://doi.org/10.1016/S0012-821X(99)00082-5).
4. Gucsik, A.; Koeberl, C.; Brandstatter, F.; Libowitzky, E.; Reimold, W.U. Cathodoluminescence, electron microscopy, and Raman spectroscopy of experimentally shock metamorphosed zircon crystals and naturally shocked zircon from the Ries impact crater. In *Cratering in Marine Environments and on Ice*; Dypvik, H., Burchell, M., Claeys, P., Eds.; Springer: Berlin/Heidelberg, Germany, 2004; pp. 281–322. https://doi.org/10.1007/978-3-662-06423-8_15.
5. Wittmann, A.; Kenkmann, T.; Schmitt, R.T.; Stöffler, D. Shock-metamorphosed zircon in terrestrial impact craters. *Meteorit. Planet. Sci.* **2006**, *41*, 433–454. <https://doi.org/10.1111/j.1945-5100.2006.tb00472.x>.
6. Zhang, Y. *High-Entropy Materials*; Springer Nature Singapore Pte Ltd.: Singapore, 2019; p. 152. <https://doi.org/10.1007/978-981-13-8526-1>.
7. Singleton, A.C.; Osinski, G.R.; Shieh, S.R. Microscopic effects of shock metamorphism in zircons from the Houghton impact structure, Canada. In *Special Paper of Geological Society of America*; Osinski, G.R., Kring, D.A., Eds.; Geological Society of America: Boulder, CO, USA, 2015; Volume 518, pp. 135–148. <https://doi.org/10.1130/2015.25189>.
8. Timms, N.E.; Erickson, T.M.; Pearce, M.A.; Cavosie, A.J.; Schmieder, M.; Tohver, E.; Reddy, S.M.; Zanetti, M.R.; Nemchin, A.A.; Wittmann, A. A pressure-temperature phase diagram for zircon at extreme conditions. *Earth-Sci. Rev.* **2017**, *165*, 185–202. <https://doi.org/10.1016/j.earscirev.2016.12.008>.
9. Nasdala, L.; Wenzel, M.; Vavra, G.; Irmer, G.; Wenzel, T.; Kober, B. Metamictisation of natural zircon: Accumulation versus thermal annealing of radioactivity-induced damage. *Contrib. Mineral. Petr.* **2001**, *141*, 25–144. <https://doi.org/10.1007/s004100000235>.
10. Nasdala, L.; Reiners, P.P.W.; Garver, J.I.; Kennedy, A.K.; Stern, R.A.; Balan, E.; Wirth, R. Incomplete retention of radiation damage in zircon from Sri Lanka. *Am. Mineral.* **2004**, *89*, 219–231. <https://doi.org/10.2138/am-2004-0126>.
11. Watson, E.B.; Wark, D.A.; Thomas, J.B. Crystallization thermometers for zircon and rutile. *Contrib. Mineral. Petr.* **2006**, *151*, 413–433. <https://doi.org/10.1007/s00410-006-0068-5>.
12. Hoskin, P.W.O.; Black, L.P. Metamorphic zircon formation by solid-state recrystallization of protolith igneous zircon. *J. Metamorph. Geol.* **2000**, *18*, 423–439. <https://doi.org/10.1046/j.1525-1314.2000.00266.x>.
13. Hoskin, P.W.O.; Schaltegger, U. The composition of zircon and igneous and metamorphic petrogenesis. In *Reviews in Mineralogy and Geochemistry*; Hanchar, J.M., Hoskin, P.W.O., Eds.; Mineralogical Society of America: Concord, MA, USA, 2003; Volume 53, pp. 27–62. <https://doi.org/10.2113/0530027>.
14. Kaulina, T.V. *Formation and Transformation of Zircon in Polymetamorphic Complexes*; Publishing House of Geological Institute of Kola Science Centre of the Russian Academy of Sciences: Apatity, Russia, 2010; p. 145.
15. Makeyev, A.B.; Skublov, S.G. Y-REE-rich zircons of the Timan region: Geochemistry and economic significance. *Geochem. Int.* **2016**, *54*, 788–794. <https://doi.org/10.1134/S0016702916080073>.
16. Zhang, M.; Salje, E.K.H.; Capitani, G.C.; Leroux, H.; Clark, A.M.; Schlüter, J.; Ewing, R.C. Annealing of a-decay damage in zircon: A Raman spectroscopic study. *J. Phys. Condens. Met.* **2000**, *12*, 3131–3148. <https://doi.org/10.1088/0953-8984/12/13/321>.
17. Geisler, T.; Schaltegger, U.; Tomaschek, F. Re-equilibration of zircon in aqueous fluids and melts. *Elements* **2007**, *3*, 43–50. <https://doi.org/10.2113/gselements.3.1.43>.
18. Smith, E.; Dent, G. *Modern Raman Spectroscopy: A Practical Approach*, 2nd ed.; John Wiley & Sons: Chichester, UK, 2019; p. 256.
19. Nasdala, L.; Beyssac, O.; Schopf, W.J.; Bleisteiner, B. Application of Raman-based images in the Earth Sciences. In *Springer Series in Optical Sciences*; Zoubir, A., Eds.; Springer: Berlin/Heidelberg, Germany, 2012; Volume 168, pp. 145–187. https://doi.org/10.1007/978-3-642-28252-2_5.
20. Nasdala, L.; Smith, D.C.; Kaindl, R.; Ziemann, M.A. Raman spectroscopy. In *EMU Notes in Mineralogy*; Beran, A., Libowitzky, E., Eds.; Eötvös University Press: Budapest, Hungary, 2004; Volume 6, pp. 281–343.
21. Knittle, E.; Williams, Q. High-pressure Raman spectroscopy of ZrSiO₄: Observation of the zircon to scheelite transition at 300 K. *Am. Mineral.* **1993**, *78*, 245–252.

22. Wittmann, A.; Schmitt, R.T.; Hecht, L.; Kring, D.A.; Reimold, W.U.; Povenmire, H. Petrology of impact melt rocks from the Chesapeake Bay Crater, USA. In *Special Paper of Geological Society of America*; Gohn, G.S., Koeberl, C., Miller, K.G., Reimold, W.U., Eds.; Geological Society of America: Boulder, CO, USA, 2009; Volume 458, pp. 377–396. [https://doi.org/10.1130/2009.2458\(17\)](https://doi.org/10.1130/2009.2458(17)).
23. Erickson, T.M.; Pearce, M.A.; Reddy, S.M.; Timms, N.E.; Cavosie, A.J.; Bourdet, J.; Rickard, W.D.A.; Nemchin, A.A. Microstructural constraints on the mechanisms of the transformation to reidite in naturally shocked zircon. *Contrib. Mineral. Petrol.* **2017**, *172*, 1. <https://doi.org/10.1007/s00410-016-1322-0>.
24. Cavosie, A.J.; Timms, N.E.; Erickson, T.M.; Koeberl, C. New clues from Earth's most elusive impact crater: Evidence of reidite in Australasian tektites from Thailand. *Geology* **2018**, *46*, 203–206. <https://doi.org/10.1130/G39711.1>.
25. Cavosie, A.J.; Timms, N.E.; Ferrière, L.; Rochette, P. FRIGN zircon—The only terrestrial mineral diagnostic of high-pressure and high-temperature shock deformation. *Geology* **2018**, *46*, 891–894. <https://doi.org/10.1130/G45079.1>.
26. Reddy, S.M.; Johnson, T.E.; Fischer, S.; Rickard, W.D.A.; Taylor, R.J.M. Precambrian reidite discovered in shocked zircon from the Stac Fada impactite, Scotland. *Geology* **2015**, *43*, 899–902. <https://doi.org/10.1130/G37066.1>.
27. Zamyatin, D.A.; Shchapova, Y.V.; Votyakov, S.L.; Nasdala, L.; Lenz, C.; Alteration and chemical U-Th-total Pb dating of heterogeneous high-uranium zircon from a pegmatite from the Aduiskii massif, middle Urals, Russia. *Mineral. Petrol.* **2017**, *111*, 475–497. <https://doi.org/10.1007/s00710-017-0513-3>.
28. Nasdala, L.; Irmer, G.; Wolf, D. The degree of metamictization in zircon: A Raman spectroscopic study. *Eur. J. Mineral.* **1995**, *7*, 471–478. <https://doi.org/10.1127/ejm/7/3/0471>.
29. Kovaleva, E.; Zamyatin, D.A.; Habler, G. Granular zircon from Vredefort granophyre (South Africa) confirms the deep injection model for impact melt in large impact structures. *Geology* **2019**, *47*, 691–694. <https://doi.org/10.1130/G46040.1>.
30. Kovaleva, E.; Zamyatin, D.A. Revealing microstructural properties of shocked and tectonically deformed zircon from the Vredefort impact structure: Raman spectroscopy combined with SEM microanalyses. In *Special Paper of Geological Society of America*; Reimold, W.U., Koeberl, C., Eds.; Geological Society of America: Boulder, CO, USA, 2021; Volume 550, pp. 432–448. [https://doi.org/10.1130/2021.2550\(18\)](https://doi.org/10.1130/2021.2550(18)).
31. Kolesov, B.A.; Geiger, C.A.; Armbruster, T. The dynamic properties of zircon studied by single-crystal X-ray diffraction and Raman spectroscopy. *Eur. J. Mineral.* **2001**, *13*, 939–948. <https://doi.org/10.1127/0935-1221/2001/0013-0939>.
32. Ende, M.N.; Chanmuang, C.N.; Reiners, P.W.; Zamyatin, D.A.; Sarah, E.; Gain, M.; Wirth, R.; Nasdala, L. Dry annealing of radiation-damaged zircon: Single-crystal X-ray and Raman spectroscopy study. *Lithos* **2021**, *406–407*, 106523. <https://doi.org/10.1016/j.lithos.2021.106523>.
33. Nasdala, L.; Beran, A.; Libowitzky, E.; Wolf, D. The incorporation of hydroxyl groups and molecular water in natural zircon (ZrSiO₄). *Am. J. Sci.* **2001**, *301*, 831–857. <https://doi.org/10.2475/ajs.301.10.831>.
34. Roszjar, J.; Moser, D.E.; Hyde, B.C.; Chanmuang, C.; Tait, K. Comparing chemical microstructures of some early solar system zircon from differentiated asteroids, mars and earth. In *Geophysical Monograph Series*; Moser, D.E., Corfu, F., Darling, J.R., Reddy, S.M., Tai, R., Eds.; Wiley-Blackwell: Hoboken, NJ, USA, 2017; Volume 232, pp. 113–135. <https://doi.org/10.1002/9781119227250.ch5>.
35. Page, M.J.; McKenzie, J.E.; Bossuyt, P.M.; Boutron, I.; Hoffmann, T.C.; Mulrow, C.D.; Shamseer, L.; Tetzlaff, J.M.; Akl, E.A.; Brennan, S.E. The PRISMA 2020 statement: An updated guideline for reporting systematic reviews. *Int. J. Surg.* **2021**, *88*, 105906. <https://doi.org/10.1136/bmj.n71>.
36. Mendeleev. Available online: https://www.mendeley.com/?interaction_required=true (accessed on 29 April 2022).
37. Wopenka, B.; Jolliff, B.L.; Zinner, E.; Kremser, D.T. Trace element zoning and incipient metamictization in a lunar zircon; application of three microprobe techniques. *Am. Mineral.* **1996**, *81*, 902–912. <https://doi.org/10.2138/am-1996-7-813>.
38. Gućsik, A. Micro-Raman spectroscopy of reidite as an impact-induced high-pressure polymorph of zircon: Experimental investigation and attempt to application. *Acta Mineral. Petrogr.* **2007**, *47*, 17–24.
39. Pati, J.K.; Reimold, W.U.; Koeberl, C.; Pati, P. The Dhala structure, Bundelkhand craton, Central India—Eroded remnant of a large Paleoproterozoic impact structure. *Meteorit. Planet. Sci.* **2008**, *43*, 1383–1398. <https://doi.org/10.1111/j.1945-5100.2008.tb00704.x>.
40. Pidgeon, R.T.; Nemchin, A.A.; Kamo, S.L. Comparison of structures in zircons from lunar and terrestrial impactites. *Can. J. Earth Sci.* **2011**, *48*, 107–116. <https://doi.org/10.1139/E10-037>.
41. Zhang, A.C.; Hsu, W.B.; Li, X.H.; Ming, H.L.; Li, Q.L.; Liu, Y.; Tang, G.Q. Impact melting of lunar meteorite Dhofar 458: Evidence from polycrystalline texture and decomposition of zircon. *Meteorit. Planet. Sci.* **2011**, *46*, 103–115. <https://doi.org/10.1111/j.1945-5100.2010.01144.x>.
42. Chen, M.; Yin, F.; Li, X.; Xie, X.; Xiao, W.; Tan, D. Natural occurrence of reidite in the Xiuyan crater of China. *Meteorit. Planet. Sci.* **2013**, *48*, 796–805. <https://doi.org/10.1111/maps.12106>.
43. Grange, M.L.; Nemchin, A.A.; Pidgeon, R.T. The effect of 1.9 and 1.4 Ga impact events on 4.3 Ga zircon and phosphate from an Apollo 15 melt breccia. *J. Geophys. Res.* **2013**, *118*, 2180–2197. <https://doi.org/10.1002/jgre.20167>.
44. Li, S.-S.; Keerthy, S.; Santosh, M.; Singh, S.P.; Deering, C.D.; Satyanarayanan, M.; Praveen, M.N.; Aneeshkumar, V.; Indu, G.K.; Anilkumar, Y.; et al. Anatomy of impactites and shocked zircon grains from Dhala reveals Paleoproterozoic meteorite impact in the Archean basement rocks of Central India. *Gondwana Res.* **2018**, *54*, 81–101. <https://doi.org/10.1016/j.gr.2017.10.006>.

45. McGregor, M.; McFarlane, C.R.M.; Spray, J.G. In situ LA-ICP-MS apatite and zircon U–Pb geochronology of the Nicholson Lake impact structure, Canada: Shock and related thermal effects. *Earth Planet. Sci. Lett.* **2018**, *504*, 185–197. <https://doi.org/10.1016/j.epsl.2018.10.006>.
46. Pidgeon, R.T.; Merle, R.E.; Grange, M.L.; Nemchin, A.A. Annealing history of zircons from Apollo 14083 and 14303 impact breccias. *Meteorit. Planet. Sci.* **2018**, *53*, 2632–2643. <https://doi.org/10.1111/maps.13185>.
47. Pati, J.K.; Poelchau, M.H.; Reimold, W.U.; Nakamura, N.; Kuriyama, Y.; Singh, A.K. Documentation of shock features in impactites from the Dhala impact structure, India. *Meteorit. Planet. Sci.* **2019**, *54*, 2312–2333. <https://doi.org/10.1111/maps.13369>.
48. Walton, E.L.; Timms, N.E.; Hauck, T.E.; MacLagan, E.A.; Herd, C.D.K. Evidence of impact melting and post-impact decomposition of sedimentary target rocks from the Steen River impact structure, Alberta, Canada. *Earth Planet. Sci. Lett.* **2019**, *515*, 173–186. <https://doi.org/10.1016/j.epsl.2019.03.015>.
49. Xing, W.; Lin, Y.; Zhang, C.; Zhang, M.; Hu, S.; Hofmann, B.A.; Sekine, T.; Xiao, L.; Gu, L. Discovery of reidite in the lunar meteorite Sayh al Uhaymir 169. *Geophys. Res. Lett.* **2020**, *47*, e2020GL089583. <https://doi.org/10.1029/2020GL089583>.
50. Kaulina, T.V.; Nerovich, L.I.; Il'chenko, V.L.; Lialina, L.M.; Kunakkuzin, E.L.; Ganninbal, M.A.; Mudruk, S.V.; Elizarov, D.V.; Borisenko, E.S. Astroblems in the Early Earth History: Precambrian Impact Structures of the Kola-Karelian Region (East Baltic Shield). In *Geological and Geo-Environmental Processes on Earth*; Shandilya, A.K., Singh, V.K., Bhatt, S.C., Dubey, C.S., Eds.; Springer: Singapore, 2021; pp. 25–37. https://doi.org/10.1007/978-981-16-4122-0_3.
51. McGregor, M.; Erickson, T.M.; Spray, J.G.; Whitehouse, M.J. High-resolution EBSD and SIMS U–Pb geochronology of zircon, titanite, and apatite: Insights from the Lac La Moinerie impact structure, Canada. *Contrib. Mineral. Petrol.* **2021**, *176*, 76. <https://doi.org/10.1007/s00410-021-01828-y>.
52. Wittmann, A.; Cavosie, A.J.; Timms, N.E.; Ferrière, L.; Rae, A.; Rasmussen, C.; Ross, C.; Stockli, D.; Schmieder, M.; Kring, D.A.; et al. Shock impedance amplified impact deformation of zircon in granitic rocks from the Chicxulub impact crater. *Earth Planet. Sci. Lett.* **2021**, *575*, 117201. <https://doi.org/10.1016/j.epsl.2021.117201>.
53. Huidobro, J.; Aramendia, J.; Arana, G.; Madariaga, J.M. Geochemical Characterization of the NWA 11273 Lunar Meteorite Using Nondestructive Analytical Techniques: Original, Shocked, and Alteration Mineral Phases. *ACS Earth Space Chem.* **2021**, *5*, 1333–1342. <https://doi.org/10.1021/acsearthspacechem.0c00329>.
54. Tartèse, R.; Endley, S.; Joy, K.H. U–Pb dating of zircon and monazite from the uplifted Variscan crystalline basement of the Ries impact crater. *Meteorit. Planet. Sci.* **2022**, *54*, 830–849. <https://doi.org/10.1111/maps.13798>.
55. Dawson, P.; Hargreave, M.M.; Wilkinson, G.R. The vibrational spectrum of zircon (ZrSiO₄). *J. Phys. C. Solid. State.* **1971**, *4*, 240–256. <https://doi.org/10.1088/0022-3719/4/2/014>.
56. Zhang, M.; Boatner, L.A.; Salje, E.K.; Ewing, R.C.; Daniel, P.; Weber, W.J.; Zhang, Y.; Farnan, I. Micro-Raman and micro-infrared spectroscopic studies of Pb- and Au-irradiated ZrSiO₄: Optical properties, structural damage, and amorphization. *Phys. Rev. B* **2008**, *77*, 144110. <https://doi.org/10.1103/PhysRevB.77.144110>.
57. Griffith, W.P. Raman studies on rock-forming minerals. Part I. Orthosilicates and cyclosilicates. *J. Chem. Soc. A* **1969**, *9*, 1372–1377. <https://doi.org/10.1039/J19690001372>.
58. Geisler, T.; Rashwan, A.A.; Rahn, M.K.W.; Poller, U.; Zwingmann, H.; Pidgeon, R.T.; Schleicher, H.; Tomaschek, F. Low-temperature hydrothermal alteration of natural metamict zircons from the Eastern Desert, Egypt. *Mineral. Mag.* **2003**, *67*, 485–508. <https://doi.org/10.1180/0026461036730112>.
59. Moser, D.E.; Cupelli, C.L.; Barker, I.R.; Flowers, R.M.; Bowman, J.R.; Wooden, J.; Hart, J.R. New zircon shock phenomena and their use for dating and reconstruction of large impact structures revealed by electron nanobeam (EBSD, CL, EDS) and isotopic U–Pb and (U–Th)/He analysis of the Vredefort dome. *Can. J. Earth Sci.* **2011**, *48*, 117–139. <https://doi.org/10.1139/E11-011>.
60. Kovaleva, E.; Klötzli, U.; Habler, G.; Huet, B.; Guan, Y.; Rhede, D. The effect of crystal-plastic deformation on isotope and trace element distribution in zircon: Combined BSE, CL, EBSD, FEG-EMP and NanoSIMS study. *Chem. Geol.* **2017**, *450*, 183–198. <https://doi.org/10.1016/j.chemgeo.2016.12.030>.
61. Corfu, F.; Hanchar, J.M.; Hoskin, P.W.O.; Kinny, P. Atlas of zircon textures. In *Reviews in Mineralogy and Geochemistry*; Hanchar, J.M., Hoskin, P.W.O., Eds.; Mineralogical Society of America: Concord, MA, USA, 2003; Volume 53, pp. 469–500. <https://doi.org/10.2113/0530469>.
62. Hoskin, P. Patterns of chaos: Fractal statistics and the oscillatory chemistry of zircon. *Geochim. Cosmochim. Acta.* **2000**, *64*, 1905–1923. [https://doi.org/10.1016/S0016-7037\(00\)00330-6](https://doi.org/10.1016/S0016-7037(00)00330-6).
63. Nasdala, L.; Kronz, A.; Hanchar, J.M.; Tichomirowa, M.; Davis, D.W.; Hofmeister, W. Effects of natural radiation damage on back-scattered electron images of single crystals of minerals. *Am. Mineral.* **2006**, *91*, 1739–1746. <https://doi.org/10.2138/am.2006.2241>.
64. Ginster, U.; Reiners, P.W.; Nasdala, L.; Chanmuang, C.N. Annealing kinetics of radiation damage in zircon. *Geochim. Cosmochim. Acta.* **2019**, *249*, 225–246. <https://doi.org/10.1016/j.gca.2019.01.033>.
65. Palenik, C.S.; Nasdala, L.; Ewing, R.C. Radiation damage in zircon. *Am. Mineral.* **2003**, *88*, 770–781. <https://doi.org/10.2138/am-2003-5-606>.
66. Murakami, T.; Chakoumakos, B.C.; Ewing, R.C.; Lumpkin, G.R.; Weber, W.J. Alpha-decay event damage in zircon. *Am. Mineral.* **1991**, *76*, 1510–1532.
67. Ewing, R.C.; Weber, W.J.; Corrales, L.R. Radiation effects in zircon. In *Reviews in Mineralogy and Geochemistry*; Hanchar, J.M., Hoskin, P.W.O., Eds.; Mineralogical Society of America: Concord, MA, USA, 2003; Volume 53, pp. 387–425. <https://doi.org/10.2113/0530387>.

68. Salje, E.K.H.; Chrosch, J.; Ewing, R.C. Is “metamictization” of zircon a phase transition? *Am. Mineral.* **1999**, *84*, 1107–1116. <https://doi.org/10.2138/am-1999-7-813>.
69. Shchapova, Y.V.; Zamyatin, D.A.; Votyakov, S.L.; Zhidkov, I.S.; Kuharenko, A.I.; Cholakh, S.O. Short-range order and electronic structure of radiation-damaged zircon according to X-ray photoelectron spectroscopy. *Phys. Chem. Miner.* **2020**, *47*, 51. <https://doi.org/10.1007/s00269-020-01120-8>.
70. Zamyatin, D.A.; Votyakov, S.L.; Shchapova, Y.V. JPD-analysis as a new approach for studying the zircon texture with micron spatial resolution and its application to geochronology. *Dokl. Earth Sci.* **2019**, *486*, 376–380. <https://doi.org/10.31857/s0869-56524854479-483>.
71. Kusaba, K.; Syono, Y.; Kikuchi, M.; Fukuoka, K. Shock behaviour of zircon: Phase transition to scheelite structure and decomposition. *Earth Planet. Sci. Lett.* **1985**, *72*, 433–439. [https://doi.org/10.1016/0012-821X\(85\)90064-0](https://doi.org/10.1016/0012-821X(85)90064-0).
72. Gucsik, A.; Koeberl, C.; Brandstätter, F.; Reimold, W.U.; Libowitzky, E. Cathodoluminescence, electron microscopy, and Raman spectroscopy of experimentally shock-metamorphosed zircon. *Earth Planet. Sci. Lett.* **2002**, *202*, 495–509. [https://doi.org/10.1016/S0012-821X\(02\)00754-9](https://doi.org/10.1016/S0012-821X(02)00754-9).
73. Gucsik, A.; Zhang, M.; Koeberl, C.; Salje, E.K.H.; Redfern, S.A.T.; Pruneda, J.M. Infrared and Raman spectra of ZrSiO₄ experimentally shocked at high pressures. *Mineral. Mag.* **2004**, *68*, 801–811. <https://doi.org/10.1180/0026461046850220>.
74. El Goresy, A. Baddeleyite and its significance in impact glasses. *J. Geophys. Res.* **1965**, *70*, 3453–3456. <https://doi.org/10.1029/jz070i014p03453>.
75. Kovaleva, E.; Kusiak, M.A.; Kenny, G.G.; Whitehouse, M.J.; Habler, G.; Schreiber, A.; Wirth, R. Nano-scale investigation of granular neoblastic zircon, Vredefort impact structure, South Africa: Evidence for complete shock melting. *Earth Planet. Sci. Lett.* **2021**, *565*, 116948. <https://doi.org/10.1016/j.epsl.2021.116948>.
76. Launer, P.J. Regularities in the infrared absorption spectra of silicate minerals. *Am. Mineral.* **1952**, *37*, 764–784.
77. Saksena, V.D. Infrared absorption studies of some silicate structures. *Trans. Faraday Soc.* **1961**, *57*, 242–258.
78. Timms, N.E.; Pearce, M.A.; Erickson, T.M.; Cavosie, A.J.; Rae, A.S.P.; Wheeler, J.; Wittmann, A.; Ferrière, L.; Poelchau, M.H.; Tomioka, N.; et al. New shock microstructures in titanite (CaTiSiO₅) from the peak ring of the Chicxulub impact structure, Mexico. *Contrib. Mineral. Petrol.* **2019**, *174*, 38. <https://doi.org/10.1007/s00410-019-1565-7>.
79. Kamo, S.L.; Reimold, W.U.; Krogh, T.E.; Colliston, W.P. A 2.023 Ga age for the Vredefort impact event and a first report of shock metamorphosed zircons in pseudotachylitic breccias and Granophyre. *Earth Planet. Sci. Lett.* **1996**, *144*, 369–387. [https://doi.org/10.1016/S0012-821X\(96\)00180-X](https://doi.org/10.1016/S0012-821X(96)00180-X).
80. Aberg, G.; Bollmark, B. Retention of U and Pb in zircons from shocked granite in the Siljan impact structure, Sweden. *Earth Planet. Sci. Lett.* **1985**, *74*, 347–349. [https://doi.org/10.1016/S0012-821X\(85\)80006-6](https://doi.org/10.1016/S0012-821X(85)80006-6).
81. Deutsch, A.; Schärer, U. Isotope systematics and shock-wave metamorphism: I. U-Pb in zircon, titanite and monazite, shocked experimentally up to 59 GPa. *Geochim. Cosmochim. Acta* **1990**, *54*, 3427–3434. [https://doi.org/10.1016/0016-7037\(90\)90295-V](https://doi.org/10.1016/0016-7037(90)90295-V).
82. Bohor, B.F.; Betterton, W.J.; Krogh, T.E. Impact-shocked zircons: Discovery of shock-induced textures reflecting increasing degrees of shock metamorphism. *Earth Planet. Sci. Lett.* **1993**, *119*, 419–424. [https://doi.org/10.1016/0012-821X\(93\)90149-4](https://doi.org/10.1016/0012-821X(93)90149-4).
83. Deloule, E.; Chaussidon, M.; Glass, B.P.; Koeberl, C. U–Pb isotopic study of relict zircon inclusions recovered from Muong Nong-type tektites. *Geochim. Cosmochim. Acta* **2001**, *65*, 1833–1838. [https://doi.org/10.1016/S0016-7037\(01\)00548-8](https://doi.org/10.1016/S0016-7037(01)00548-8).
84. Grange, M.L.; Pidgeon, R.T.; Nemchin, A.A.; Timms, N.E.; Meyer, C. Interpreting U–Pb data from primary and secondary features in lunar zircon. *Geochim. Cosmochim. Acta* **2013**, *101*, 112–132. <https://doi.org/10.1016/j.gca.2012.10.013>.
85. Kleinmann, B. The breakdown of zircon observed in the Libyan desert glass as evidence of its impact origin. *Earth Planet. Sci. Lett.* **1968**, *5*, 497–501. [https://doi.org/10.1016/s0012-821x\(68\)80085-8](https://doi.org/10.1016/s0012-821x(68)80085-8).
86. Joy, K.H.; Snape, J.F.; Nemchin, A.A.; Tartèse, R.; Martin, D.M.; Whitehouse, M.J.; Vishnyakov, V.; Pernet-Fisher, J.F.; Kring, D.A. Timing of geological events in the lunar highlands recorded in shocked zircon-bearing clasts from Apollo 16: Shocked zircon from Apollo 16. *Roy. Soc. Open Sci.* **2020**, *7*, 200236. <https://doi.org/10.1098/rsos.200236>.